Homogenization theory for periodic distributions of elastic cylinders embedded in a viscous fluid

Edgar Reyes-Ayona, Daniel Torrent, and José Sánchez-Dehesa[a]
Grupo de Fenómenos Ondulatorios, Universitat Politècnica de València, Camino de Vera s.n. (Edificio 7F), ES-46022 Valencia, Spain

A multiple-scattering theory is applied to study the homogenization of clusters of elastic cylinders distributed in a isotropic lattice and embedded in a viscous fluid. Asymptotic relations are derived and employed to obtain analytical formulas for the effective parameters of homogenized clusters in which the underlying lattice has a low filling fraction. It is concluded that such clusters behave, in the low frequency limit, as an effective elastic medium. Particularly, it is found that the effective dynamical mass density follows the static estimate; i.e., the homogenization procedure does not recover the non-linear behavior obtained for the inviscid case. Moreover, the longitudinal and transversal sound speeds do not show any dependence on fluid viscosity. Numerical simulations performed for clusters made of brass cylinders embedded in glycerin support the reliability of the effective parameters resulting from the homogenization procedure reported here.
© 2012 Acoustical Society of America. [http://dx.doi.org/10.1121/1.4744933]

I. INTRODUCTION

The propagation of acoustic waves in inhomogeneous media has attracted much attention over the years. Recently, there has been a growing interest in a special type of inhomogeneous materials named phononic crystals, whose elastic parameters vary periodically in space. The interest in these materials arises from the possibility of having frequency regions, known as absolute band gaps, where the propagation of elastic waves is forbidden, whatever their polarization and wave vector.[1–5] In addition to their ability to behave like perfect mirrors, these structures can prove particularly useful for applications requiring a spatial confinement of acoustic waves and can hence be used as acoustic filters or very efficient waveguides.[5] A class of phononic crystals where the solid background is replaced by a fluid or a gas are usually called sonic crystals.[6–8]

The theoretical description of sonic and phononic crystals has employed two main strategies. One consists of band structure calculations[1–4,6–8] of the corresponding infinite system in order to match the gaps in the dispersion relation with the attenuations found in the transmission spectra. The other one calculates the transmission spectra by different algorithms such as the transfer matrix method,[9] finite differences,[10–12] or by multiple scattering.[13–15] The latter is the most suitable for describing finite-size structures. Experimental observations have recently demonstrated that phononic crystals can also be employed in the frequency region well below the bandgap as acoustic lenses for sound focusing as well as acoustic interferometers that work similarly to their optical counterparts.[16,17] Inspired by these findings, several approaches have been presented in order to give a description of phononic crystals in the low frequency limit or long

wavelengths.[18–28] Kafesaki *et al.*[18] analyzed the phenomenon of the sound speed of drops in mixtures by means of an effective medium obtained by using the coherent potential approximation. Krokhin *et al.*[19] employed plane wave expansions to derive analytical expressions for the speed of sound valid for arbitrary filling fraction and different geometries of the inclusions. More recently Mei *et al.*[24] and Torrent *et al.*[25,26] applied the multiple scattering method to develop a homogenization theory to simultaneously obtain the effective sound speed as well as the effective density of finite cluster of cylinders embedded in air. Kutsenko *et al.*[27] introduced a new analytical approach based on the monodromy matrix for the two dimensional case to derive the effective shear speed in two dimensional phononic crystals. Finally, the results of Wu and co-workers[28] are also of interest to this work though they report an effective medium theory applied to the case of elastic inclusions embedded in a different elastic medium.

Despite of the extensive studies in sonic/phononic crystals the effect of losses at low frequencies has been scarcely considered. Only a few works have been devoted to this topic. A related problem was firstly tackled by Einstein in his classical 1905 paper, where he studied the effective viscosity of rigid spheres in a viscous medium.[29] Afterwards, Batchelor and Green[30] tried to determine the bulk stress in a suspension of spherical particles up the second order in the filling fraction and Sprik and Wegdam[31] showed that shear viscosity in the liquid constituent may lead to gap formation in solid-liquid systems. For the case of periodic distributions, Psarobas *et al.*[32,33] developed an on-shell multiple scattering method in order to incorporate the effect of viscoelastic losses in the band structure calculation by means of a complex and dispersive Lamé's constant. Hussein[34,35] introduced a modified finite element method (reduced Bloch mode expansion) to calculate the dispersion relation using finite-number set of Bloch mode eigenvectors at each wave-vector point.

[a]Author to whom correspondence should be addressed. Electronic mail: jsdehesa@upvnet.upv.es

It was found that in sonic crystals the existence of complete band gap is more difficult due to suppression of transversal sound in the liquid background. However, viscosity in liquids may lead to gap formation in solid-liquid systems. Shear viscosity in the liquid introduces a new length scale associated with the penetration of shear stress into the viscous liquid. When the viscous penetration depth $\delta = \sqrt{(2\eta/\rho_b\omega)}$ becomes comparable to the structural length scale in the composite, viscous effects cannot be ignored in describing the acoustical properties.

In this work we analyze the scattering of acoustic waves by clusters of elastic cylinders distributed in a periodic lattice and immersed in a viscous medium. We are here interested in the homogenization of this type of systems and their properties are obtained using an effective medium theory. In other words, we are considering clusters interacting with sound wavelengths much larger than the distance between cylinders and larger also than the cylinder's diameter size. In terms of frequencies, we are dealing with very low frequencies; i.e., in a frequency region very far from the frequency at which the first acoustic band gap of the underlying lattice appears. Asymptotic relations are derived and employed to formulate a method of homogenization based on the scattering properties of the cluster. By using the multiple-scattering method we have demonstrated that, in the long wavelength limit, a distribution of elastic cylinders embedded in a viscous fluid effectively behaves like a single elastic cylinder with parameters that can be analytically obtained. Semi-analytical formulas for the effective parameters (i.e., effective longitudinal sound speed, effective transversal sound speed, and effective density) are obtained in the case of dilute (low filling fraction) structures. We have obtained that the effective mass density follows the linear static estimate, that is, the homogenization procedure does not recover an effective mass density with a non-linear dependence on the filling fraction, as was the result for the inviscid case. Moreover, it is worth mentioning that there is no explicit dependence on the fluid viscosity for the mass density or for the longitudinal and transversal sound speeds. However, viscosity effects are implicitly involved in the resulting effective parameters through the boundary conditions employed in the homogenization procedure.

This article is organized as follows. In Sec. II the mathematical formulation for a single elastic cylinder in a viscous background is introduced and the generalization to the case of a cluster by using the multiple scattering method is also briefly described. In Sec. III the concept of effective t matrix is introduced and the effective parameters are obtained for a general elastic-viscous fluid composite. Numerical results for a single and a cluster of elastic cylinders embedded in a viscous fluid are reported and discussed in Sec. IV, where the limit of wavelength to reach homogenization behavior in these systems is also studied as a function of the frequency. Finally, the work is summarized in Sec. V.

II. MATHEMATICAL FORMULATION

There are a wide variety of models in the literature that deal with viscous effects in acoustic wave propagation. The model most commonly used, which is also followed here, is based on the solution of the mechanical equations; i.e., all the terms in the linearized Navier–Stokes equations are taken into account. This particular treatment of viscosity complicates the analysis because the fluid medium can uphold shear and compressional modes; both must be accounted for satisfying the boundary conditions at the interfaces. First, we theoretically examine the two-dimensional (2D) scattered acoustic field produced by an impinging plane wave on a single elastic solid cylinder in order to obtain the t matrix. We assume, without loss of generality, that the cylinder has a circular cross-section and that it is infinitely long along the z-axis. We also consider that the incident wave propagates normally to the cylinder axis. Then we generalize the result to the case of multiple scatterers of arbitrary cross section.

A. t matrix of an elastic cylinder embedded in a viscous medium

Let us consider the standard acoustic equations for linear flows in a homogeneous viscous fluid medium; i.e., the equation of continuity

$$\frac{\partial \rho}{\partial t} + \rho_b \nabla \cdot \mathbf{v} = 0, \tag{1}$$

the momentum equation

$$\nabla p + \rho_b \frac{\partial \mathbf{v}}{\partial t} = \eta \nabla^2 \mathbf{v} + \left(\xi + \frac{1}{3}\eta\right)\nabla(\nabla \cdot \mathbf{v}), \tag{2}$$

and the equation of state

$$\frac{dp}{d\rho} = c_b^2, \tag{3}$$

in which $\mathbf{v}$ is the complex fluid velocity vector, ρ_b is the ambient fluid density, ρ is the density perturbation, p is the fluid pressure, c_b is the sound speed, and η and ξ are the shear and bulk viscosities, respectively.

Equations (1)–(3) can be combined to obtain the equation for the velocity vector $\mathbf{v}$:

$$\rho_b \frac{\partial^2 \mathbf{v}}{\partial t^2} - \rho_b c_b^2 \nabla(\nabla \cdot \mathbf{v}) = \eta \nabla^2 \frac{\partial \mathbf{v}}{\partial t} + \left(\xi + \frac{1}{3}\eta\right)\nabla\left(\nabla \cdot \frac{\partial \mathbf{v}}{\partial t}\right). \tag{4}$$

The velocity field can be expressed as a superposition of longitudinal and transversal vector components by using the Helmholtz decomposition theorem,

$$\mathbf{v} = -\nabla \varphi + \nabla \times \psi, \tag{5}$$

where φ and ψ are the scalar and vector potentials, respectively. For 2D periodicity the vector potential has only z-component, $\psi = (0, 0, \psi)$. Now, substituting this decomposition into Eq. (4), we get the following two equations:

$$(\nabla^2 + k_\ell^2)\varphi = 0,$$
$$(\nabla^2 + k_t^2)\psi = 0, \tag{6}$$

J. Acoust. Soc. Am., Vol. 132, No. 4, Pt. 2, October 2012

Reyes-Ayona *et al.*: Homogenization of rods in a viscous fluid   2897

where k_ℓ and k_t are the longitudinal and transversal wave numbers, respectively, in the viscous fluid and are given by

$$k_\ell = \frac{\omega}{c_b}\left[1 + i\frac{\omega}{2\rho_b c_b^2}\left(\frac{4}{3}\eta + \xi\right)\right],$$
$$k_t = (1 + i)\sqrt{\frac{\omega\rho_b}{2\eta}}. \tag{7}$$

The solutions of Eq. (6) are obtained by expanding the longitudinal and transversal vector components in series of Bessel (Hankel) functions as follows:

$$\varphi_{\text{ext}} = \sum_{q=-\infty}^{\infty} A_q^\ell J_q(k_\ell r)e^{iq\theta}, \tag{8}$$

and

$$\varphi_{\text{scatt}} = \sum_{q=-\infty}^{\infty} B_q^\ell H_q(k_\ell r)e^{iq\theta},$$
$$\psi_{\text{scatt}} = \sum_{q=-\infty}^{\infty} B_q^t H_q(k_t r)e^{iq\theta}. \tag{9}$$

The field φ_{ext} represents the incident (external) field over the cylinder while φ_{scatt} and ψ_{scatt} are the respective components of the scattered fields. The expansion over Hankel functions only guarantees that the scattered waves are outgoing. We also assume that the external field is pure longitudinal; i.e., the background considered here is a viscous fluid that, in absence of scatterers, supports propagation of longitudinal waves only.

On the other hand, sound wave in the elastic cylinder is described by the equation for the displacement vector (Navier's equation of elasticity):

$$\rho_a \frac{\partial^2 \mathbf{u}}{\partial t^2} = (\lambda_a + \mu_a)\nabla(\nabla \cdot \mathbf{u}) + \mu_a \nabla^2 \mathbf{u}, \tag{10}$$

where ρ_a, λ_a, and μ_a are the density and the Lamé's constants of the cylinder, respectively. The displacement vector is related to the velocity vector by means of the temporal derivative, $\mathbf{v} = \partial\mathbf{u}/\partial t = -i\omega\mathbf{u}$. Introducing scalar and vector potential for velocity $\mathbf{v}$, we obtain

$$v_r = -i\omega\left(-\frac{\partial\phi}{\partial r} + \frac{1}{r}\frac{\partial\zeta}{\partial\theta}\right),$$
$$v_\theta = i\omega\left(\frac{1}{r}\frac{\partial\phi}{\partial\theta} + \frac{\partial\zeta}{\partial r}\right). \tag{11}$$

Here the potentials ϕ and ζ can be analogously expanded over Bessel functions

$$\phi_{\text{int}} = \sum_{q=-\infty}^{\infty} C_q^\ell J_q(k_\ell^a r)e^{iq\theta},$$
$$\zeta_{\text{int}} = \sum_{q=-\infty}^{\infty} C_q^t J_q(k_t^a r)e^{iq\theta}, \tag{12}$$

where $k_\ell^a = \omega/c_\ell$ and $k_\ell^a = \omega/c_t$ are the longitudinal and transversal wave vectors, respectively, and c_ℓ and c_t their corresponding velocities, which are given in terms of mass density and Lamé's constants.

The coefficients of expansions (9) and (12) are obtained by imposing the continuity of the normal and tangential components of the velocity and stresses, respectively, at the cylinder surface. After some algebra, we get the t matrix that relates the coefficients A_q^ℓ to B_q^ℓ and B_q^t is (see Appendix A)

$$\mathbf{t}_q = -[\mathbf{Q_q} - \mathbf{R_q O_q^{-1} N_q}]^{-1}[\mathbf{P_q} - \mathbf{R_q O_q^{-1} M_q}]. \tag{13}$$

In general the t-matrix is a block diagonal matrix whose diagonal elements $\mathbf{t}_q$ are 2×2 matrices

$$\mathbf{t}_q = \begin{pmatrix} t_q^{\ell\ell} & t_q^{\ell t} \\ t_q^{t\ell} & t_q^{tt} \end{pmatrix}, \tag{14}$$

where $t_q^{\ell\ell}$ and $t_q^{t\ell}$ involved Bessel and Hankel functions, and $t_q^{\ell t}$ and t_q^{tt} are equal to zero (see Appendix A). Note that even when determinant of the t-matrix is zero the flux conservation is satisfied. Elasticity involves the existence of two polarization modes so that the conservation of flux implies the conservation of the total flux; i.e., the addition of the longitudinal and transversal fluxes instead of conservation of individual components.

Let us recall that the problem of a single elastic cylinder in a viscous fluid has been already considered in Refs. 36 and 37 for circular and elliptic cross sections, respectively. In these studies the coefficients B_q^ℓ and B_q^t are obtained from A_q^ℓ by solving a system of linear equations. However, here we have developed a t matrix formalism in order to tackle the problem of multiple elastic cylinders in a cluster. For a comprehensive description of this formalism and its application to problems of multiple scattering the readers are addressed to the book by Varadan and Varadan,[38] and the references therein.

B. Sound scattering by a cluster of elastic cylinders embedded in a viscous medium

Now, let us consider a cluster of N cylinders located at positions $\mathbf{R}_\beta$ ($\beta = 1, 2, ..., N$), $\mathbf{R}_\beta$ is a vector in the XY plane. The cylinders will be assumed of arbitrary cross section. The geometry of the problem and the definitions of the variable employed are shown in Fig. 1.

If an external wave φ^{ext} with temporal dependence $e^{-i\omega t}$ impinges the cluster, the total field around a cylinder α is a superposition of the external field and the radiation scattered by the rest of the cylinders β:

$$\varphi_\alpha(r, \theta) = \varphi^{\text{ext}}(r, \theta) + \sum_{\beta\neq\alpha}^{N} \varphi_\beta^{\text{scatt}}(r, \theta),$$
$$\psi_\alpha(r, \theta) = \sum_{\beta\neq\alpha}^{N} \psi_\beta^{\text{scatt}}(r, \theta), \tag{15}$$

where $\varphi_\beta^{\text{scatt}}$ and $\psi_\beta^{\text{scatt}}$ are the fields scattered by the β cylinder. Without loss of generality, those fields can be expanded
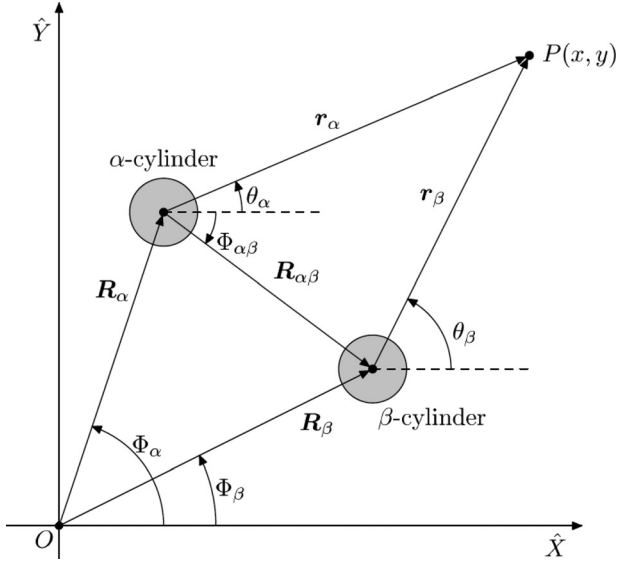
FIG. 1. Coordinate systems and definition of variables employed in the equations of the multiple-scattering.

as a combination of Bessel and Hankel functions centered at the cylinder position. If the expansion coefficients are $(C_\alpha)_q^\ell$, $(A_\alpha)_q^\ell$, $(B_\beta)_q^\ell$, $(C_\alpha)_q^t$, and $(B_\beta)_q^t$, for φ_α, φ^{ext}, $\varphi_\beta^{\text{scatt}}$, ψ_α, and $\psi_\beta^{\text{scatt}}$, respectively, the expressions (15) can be cast into the following relations between the coefficients:

$$(C_\alpha)_q^\ell = (A_\alpha)_q^\ell + \sum_{\beta\neq\alpha}^{N}\sum_{s=-\infty}^{\infty}(G_{\alpha\beta}(k_\ell))_{qs}(B_\beta)_s^l,$$

$$(C_\alpha)_q^t = \sum_{\beta=1}^{N}\sum_{s=-\infty}^{\infty}(G_{\alpha\beta}(k_t))_{qs}(B_\beta)_s^t; \qquad (16)$$

$(G_{\alpha\beta}(k_i))_{qs}$ being the propagator from β to α whose components are

$$(G_{\alpha\beta}(k_i))_{qs} = (1-\delta_{\alpha\beta})e^{i(s-q)\Phi_{\alpha\beta}}H_{q-s}(k_i r_{\alpha\beta}), \qquad (17)$$

for $k_i = k_\ell, k_t$.

Note that coefficients $(A_\alpha)_q^\ell$ in Eq. (16) are known, but $(C_\alpha)_q^\ell$, $(B_\beta)_q^\ell$, $(C_\alpha)_q^t$, and $(B_\beta)_q^t$ are not. To reduce the complexity of the following calculations it is convenient to express Eq. (16) in a more compact way, i.e.,

$$(c_\alpha)_q = (a_\alpha)_q + \sum_{\beta=1}^{N}\sum_{s=-\infty}^{\infty}(\mathbf{G}_{\alpha\beta})_{qs}(\mathbf{b}_\beta)_s, \qquad (18)$$

with

$$(c_\alpha)_q = \begin{pmatrix}(C_\alpha)_q^\ell \\ (C_\alpha)_q^t\end{pmatrix}; \quad (\mathbf{b}_\beta)_s = \begin{pmatrix}(B_\beta)_s^\ell \\ (B_\beta)_s^t\end{pmatrix};$$

$$(\mathbf{a}_\alpha)_q = \begin{pmatrix}(A_\alpha)_q^\ell \\ 0\end{pmatrix}$$

and

$$(\mathbf{G}_{\alpha\beta})_{qs} = \begin{pmatrix}(G_{\alpha\beta}(k_\ell))_{qs} & 0 \\ 0 & (G_{\alpha\beta}(k_t))_{qs}\end{pmatrix}. \qquad (19)$$

As in the case of a single cylinder, the boundary conditions at the cylinder surface allow us to calculate the t matrix whose components $(\mathbf{t}_\alpha)_{qs}$ relate the coefficients $(\mathbf{c}_\alpha)_q$ and $(\mathbf{b}_\beta)_s$:

$$(\mathbf{b}_\alpha)_s = \sum_q (\mathbf{t}_\alpha)_{qs}(\mathbf{c}_\alpha)_s. \qquad (20)$$

Introducing the coefficients (20) in Eq. (18), after straight-forward calculation we get

$$(\mathbf{b}_\alpha)_q - \sum_{\beta=1}^{N}\sum_{s=-\infty}^{\infty}(\mathbf{t}_\alpha\mathbf{G}_{\beta\alpha})_{qs}(\mathbf{b}_\beta)_s = (\mathbf{t}_\alpha\mathbf{a}_\alpha)_q. \qquad (21)$$

By truncating the sum over s within $|s| < q_{\max}$, this equation is reduced to a linear equation where the dimension of the relevant matrix is $2N(2q_{\max}+1) \times 2N(2q_{\max}+1)$. Thus, in matrix form $\mathcal{M}\mathcal{B} = \mathcal{S}$, where $\mathcal{B}$ and $\mathcal{S}$ are column block matrices with elements $(\mathbf{b}_1)_q$, $(\mathbf{b}_2)_q$,..., $(\mathbf{b}_N)_q$, and $(\mathbf{t}_1\mathbf{a}_1)_q$, $(\mathbf{t}_2\mathbf{a}_2)_q$,..., $(\mathbf{t}_N\mathbf{a}_N)_q$, respectively. $\mathcal{M}$ is a $N \times N$ block matrix where each element is a matrix of dimension $2(2q_{\max}+1) \times 2(2q_{\max}+1)$. In short, the matrix elements can be expressed by

$$(\mathbf{M}_{\alpha\beta})_{qs} = \delta_{\alpha\beta}\delta_{qs}\mathbf{I} - (\mathbf{t}_\alpha\mathbf{G}_{\alpha\beta})_{qs}. \qquad (22)$$

Finally, the unknown coefficients $\mathcal{B}$ can be easily obtained by a matrix inversion, $\mathcal{B} = \mathcal{M}^{-1}\mathcal{S}$:

$$(\mathbf{b}_\alpha)_q = \sum_{\beta=1}^{N}\sum_{s=-\infty}^{\infty}(\mathbf{M}_{\alpha\beta}^{-1})_{qs}(\mathbf{t}_\beta\mathbf{a}_\beta)_s. \qquad (23)$$

Thus the solution for a given cluster is obtained in terms of the block matrix $(\mathbf{M}_{\alpha\beta}^{-1})_{qs}$ and the t matrix of the individual cylinders. As explained before, the t matrix is diagonal as in the inviscid case but now has a higher dimensionality since involves two different modes of propagation. This result is very general and valid for cylinders of any cross section, any filling fraction and any frequency. However, it is worth to mention that the above statement must be restricted, in the case of complex cross sections, to the possibility of evaluating the t matrix correctly and efficiently. Despite that we can assume that it is valid in general and it is particularly valid for low frequencies, which is the regime studied in the next section.

III. HOMOGENIZATION OF A CLUSTER OF ELASTIC CYLINDERS EMBEDDED IN A VISCOUS MEDIUM

The purpose here is to introduce the effective t matrix of a cluster. This t-matrix will relate the coefficients of the incident field to the coefficients of the field scattered by the cluster. The total scattered field around the cluster will be a

superposition of the fields scattered by all the cylinders, that is,

$$P^{\text{scatt}}(r,\theta) = \frac{\rho_b c_b^2}{i\omega} \nabla \cdot \mathbf{v}^{\text{scatt}}(r,\theta)$$

$$= P_0 \sum_{\alpha=1}^{N} \sum_{q=-\infty}^{\infty} (B_\alpha)_q^\ell H_q(k_\ell r_\alpha) e^{iq\theta_\alpha}, \quad (24)$$

where $H_q(\cdot)$ is the q-th order Hankel function of first kind and $(r_\alpha, \theta_\alpha)$ are the polar coordinates with the origin translated to the center of the α-cylinder, i.e., $\mathbf{r}_\alpha = \mathbf{r} - \mathbf{R}_\alpha$, as shown in Fig. 1.

The last equation can be also expressed as a function of coordinates centered at the cluster origin using the Graf's addition theorem[39] as

$$P^{\text{scatt}}(r,\theta) = P_0 \sum_{p=-\infty}^{\infty} B_p^{sc} H_p(k_\ell r) e^{ip\theta}, \quad (25)$$

where

$$B_p^{sc} = \sum_{\alpha=1}^{N} \sum_{q=-\infty}^{\infty} J_{p-q}(k_\ell R_\alpha) e^{i(q-p)\Phi_\alpha} (B_\alpha)_q^\ell. \quad (26)$$

These coefficients are related to $(A_\beta)_s^l$, or more precisely to $(\mathbf{a}_\beta)_s$, through the expression in Eq. (23) since $(B_\alpha)_q^\ell$ is the longitudinal projection of $(\mathbf{b}_\alpha)_q$, i.e., $(B_\alpha)_q^\ell = \hat{\ell} \cdot (\mathbf{b}_\alpha)_q$. Therefore,

$$B_p^{sc} = \hat{\ell} \cdot \sum_{\alpha,\beta} \sum_{q,r} J_{p-q}(k_\ell R_\alpha) e^{i(q-p)\Phi_\alpha} (\mathbf{M}_{\alpha\beta}^{-1})_{qr} (\mathbf{t}_\beta \mathbf{a}_\beta)_r. \quad (27)$$

The relationship between coefficients $(\mathbf{a}_\beta)_s$ and those of the external field $\mathbf{a}_q$ can be obtained as follows. First, we assume a generic incident field that can be expanded as a sum of Bessel functions

$$P^{\text{ext}}(r,\theta) = P_0 \sum_{q=-\infty}^{\infty} \mathbf{a}_q J_q(k_\ell r) e^{iq\theta}, \quad (28)$$

which can be expressed in terms of coordinates with origin at the α cylinder as follows:

$$P^{\text{ext}}(r_\alpha, \theta_\alpha) = P_0 \sum_{s=-\infty}^{\infty} \left(\sum_{q=-\infty}^{\infty} J_{q-s}(k_\ell R_\alpha) e^{i(q-s)\Phi_\alpha} \mathbf{a}_q \right)$$
$$\times J_s(k_\ell r_\alpha) e^{is\theta_\alpha}, \quad (29)$$

and, therefore, the coefficients $(\mathbf{a}_\alpha)_s$ are

$$(\mathbf{a}_\alpha)_s = \sum_{q=-\infty}^{\infty} J_{q-s}(k_\ell R_\alpha) e^{i(q-s)\Phi_\alpha} \mathbf{a}_q. \quad (30)$$

Now, the elements of the effective t matrix can be obtained in the following form:

$$t_{ps}^{\text{eff}} = \hat{\ell} \cdot \sum_{\alpha,\beta} \sum_{q,r,t} J_{p-q}(k_\ell R_\alpha) e^{i(q-p)\Phi_\alpha} (\mathbf{M}_{\alpha\beta}^{-1})_{qr}$$

$$\times (\mathbf{t}_\beta)_{rt} J_{s-t}(k_\ell R_\beta) e^{i(s-t)\Phi_\beta}, \quad (31)$$

which can also be cast as

$$t_{ps}^{\text{eff}} = \hat{\ell} \cdot \sum_{\alpha,\beta} \sum_{q,r,t} (\mathbf{J}_\alpha)_{pq} (\mathbf{M}_{\alpha\beta}^{-1})_{qr} (\mathbf{t}_\beta)_{rt} (\mathbf{J}'_\beta)_{st}, \quad (32)$$

where

$$(\mathbf{J}_\alpha)_{pq} = J_{p-q}(k_\ell R_\alpha) e^{i(q-p)\Phi_\alpha},$$
$$(\mathbf{J}'_\beta)_{st} = J_{s-t}(k_\ell R_\beta) e^{i(s-t)\Phi_\beta}. \quad (33)$$

When the underlying lattice of the cluster is isotropic (square or hexagonal) the cluster behaves, in the long wavelength limit, as a single homogeneous and isotropic cylinder.[40–42] Moreover, it also has been shown that the homogenization condition for a cluster of cylinders immersed in a inviscid fluid is given by[25,26]

$$\hat{t}_{pq}^{\text{eff}} = \hat{t}_{pq}^{\text{cyl}}, \quad \forall p, q, \quad (34)$$

where $\hat{t}_{pq}$ are the k-independent coefficients of the lower order terms in the k-expansion of the corresponding t-matrix elements. It is straightforward to show that, due to the form of the effective t matrix in Eq. (32), the homogenization procedure in our case of elastic cylinder in a viscous medium also leads to Eq. (34). However, as will be seen below, the effective parameters are quite different from those obtained for inviscid case.

Following the procedure employed for the inviscid case,[26] the effective parameters for a cluster of elastic cylinders embedded in a viscous fluid and distributed in a lattice with a low filling fraction are (see Appendix B):

$$\rho_{\text{eff}} = f\rho_a + (1-f)\rho_b, \quad (35a)$$

$$\frac{1}{B_{\text{eff}}} = f\frac{1}{B_a} + (1-f)\frac{1}{B_b}, \quad (35b)$$

$$\mu_{\text{eff}} = f\mu_a, \quad (35c)$$

where f is the fraction of volume occupied by the cylinders in the clusters and $B_a = \lambda_a + \mu_a$ is the 2D bulk modulus of the elastic cylinder. Note that the effective parameters do not show any explicit dependence on the viscosity for the case here considered of clusters with low f. However, the expressions have embedded the viscosity through the boundary conditions employed in their derivation. It is remarkable that the expression for ρ_{eff} in Eq. (38) is similar to that obtained from the homogenization of composites consisting of elastic inclusions embedded in another elastic medium.[28] This is an interesting result indicating that, though the boundary conditions in our system are slightly different to that of two elastic media, we arrive to similar expressions for ρ_{eff}.

Let us remark that our homogenization procedure cannot recover the effective mass density obtained for the inviscid

case, which for the case of dilute systems is $\rho_{\mathrm{eff}} = \rho_b$ $(\rho_a(1+f) + \rho_b(1-f))/(\rho_a(1-f) - \rho_b(1+f))$.[26,43–45] This can be explained as due to the fact that the inviscid case $(\eta \rightarrow 0)$ is a singular limit in the sense of the asymptotic expressions derived for the viscous medium. In order to recover the results for the inviscid case we have to return to the equation and apply the corresponding boundary conditions at the cylinders' surface. It can be concluded that the suppression of the non-linear behavior of the mass density in composites made of elastic inclusions in an elastic background and elastic bodies in a viscous background is directly related with the boundary conditions at the corresponding interfaces.

From Eq. (35) we conclude that the homogenized cylinder behaves as an effective elastic medium. Their effective longitudinal and transversal phase velocities are derived by using 2D elasticity; i.e., $c_{\ell,\mathrm{eff}} = \sqrt{(B_{\mathrm{eff}} + \mu_{\mathrm{eff}})/\rho_{\mathrm{eff}}}$ and $c_{t,\mathrm{eff}} = \sqrt{\mu_{\mathrm{eff}}/\rho_{\mathrm{eff}}}$. Their expressions are

$$\bar{c}_{\ell,\mathrm{eff}}^2 = \left(\frac{\bar{B}_a}{(1-f)\bar{B}_a + f} + f\frac{\mu_a}{B_b} \right) \left(\frac{1}{\bar{\rho}_a f + (1-f)} \right), \quad (36a)$$

$$\bar{c}_{t,\mathrm{eff}}^2 = \left(\frac{f\mu_a/B_b}{\bar{\rho}_a f + (1-f)} \right), \quad (36b)$$

where the bar symbols indicate that the magnitudes are normalized to the corresponding values of the background. In other words, the velocities are divided by c_b, and the bulk modulus and density by B_b and ρ_b, respectively. As it is shown later, these simple expressions are valid for values f as large as 0.6. A similar conclusion was reported by Parnell et al.[45] who analyzed the validity of dilute estimates in a variety of homogenization schemes applied to elastic composites. Note that an explicit dependence on the viscosity will appear for the case (not studied here) of larger f values, through the terms containing the cylinders' interaction. The case of highly compact clusters will be the object of a future work that will be published elsewhere.

Figures 2–4 depict the effective parameters (normalized to the background) as a function of filling fraction. They are obtained by analyzing clusters of N cylinders made of brass, iron (Fe), and aluminum (Al), respectively, in three different fluid backgrounds: water in Fig. 2, olive oil in Fig. 3, and glycerin in Fig. 4. We have taken $N = 151$ cylinders as representative volume element necessary to guarantee that the homogenization method produces reliable effective parameters, as it was demonstrated in the inviscid case.[25,26,39] The acoustic parameters of the three backgrounds employed in the calculations are given in Table I. The material parameters of elastic cylinders are taken to be $\rho_a = 8500 \ \mathrm{Kg/m^3}$, $c_\ell = 4305 \ \mathrm{m/s}$, $c_t = 2152 \ \mathrm{m/s}$ for brass; $\rho_a = 7870 \ \mathrm{Kg/m^3}$, $c_\ell = 5778 \ \mathrm{m/s}$, $c_t = 3137 \ \mathrm{m/s}$ for iron; $\rho_a = 2699 \ \mathrm{kg/m^3}$, $c_\ell = 6507 \ \mathrm{m/s}$, $c_t = 3044 \ \mathrm{m/s}$ for aluminum.[47] Numerical calculations are made by using these parameters normalized to that of the background, and they are summarized in Table II. The cylinders in the cluster were distributed in a hexagonal lattice whose filling fraction $f_{\mathrm{hex}} = (2\pi/\sqrt{3})(R_a/a)^2$, where a is the lattice constant. The hexagonal lattice was selected because is an isotropic lattice (like the square lattice) and for comparison purposes with the
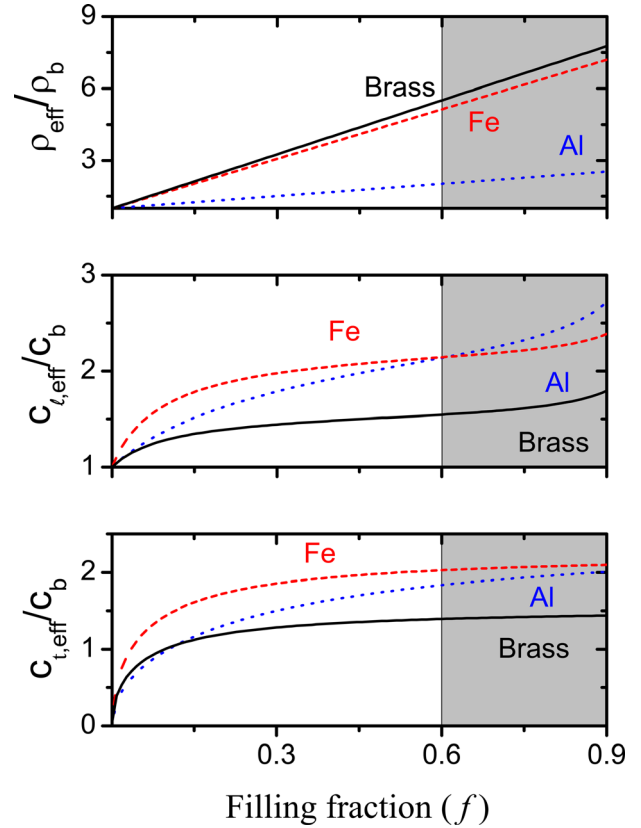

FIG. 2. (Color online) Effective parameters of composites made of cylinders of brass (continuous lines), iron (dashed lines) and aluminum (dotted lines), respectively, embedded in water as function of the filling fraction. The parameters are normalized to those of water (see Table I). The shadowed regions defined the filling fraction where the values obtained from Eqs. (35) and (36) are not reliable.

inviscid case, where results were obtained using this lattice.[25,26,48] For the calculations we have taken $a = 794 \ \mu m$ while the cylinders' radius have been changed from $R_a = 0$ to $R_a = 0.5a$, which corresponds to $0 \leq f_{\mathrm{hex}} \leq 0.907$ (close packing condition). The radius R_{eff} of the homogenized cylinder is calculated by imposing the condition

$$f_{\mathrm{cls}} = \frac{N(\pi R_a^2)}{\pi R_{\mathrm{eff}}^2} = f_{\mathrm{hex}}, \quad (37)$$

where f_{cls} is the fraction of volume occupied by the N cylinders in the cluster. For the structure under study $R_{\mathrm{eff}} = \sqrt{(N\sqrt{3}/2\pi)}a = 6.452a$.

Figures 2–4 show that $c_{\ell,\mathrm{eff}}$ is always larger than $c_{t,\mathrm{eff}}$ and that for $f \rightarrow 0$ the background properties are recovered; i.e., $c_{l,\mathrm{eff}} \rightarrow c_b$ and $c_{t,\mathrm{eff}} \rightarrow 0$.

Figure 5 shows an alternative representation of the phase velocities given in Figs. 2–4. Each point in the diagram corresponds to a filling fraction of the underlaying hexagonal lattice f_{hex}. It is observed that the effective media have ratios between longitudinal and transversal phase velocities c_ℓ/c_t that are not approximately equal or greater than 2 as in ordinary solids.[49] In fact, the ratios c_ℓ/c_t are lower than 2 and can be tailored by adjusting f_{hex}. With these new materials it is possible to get Poisson's ratios higher than 1/2 for filling fractions small enough. Recall that
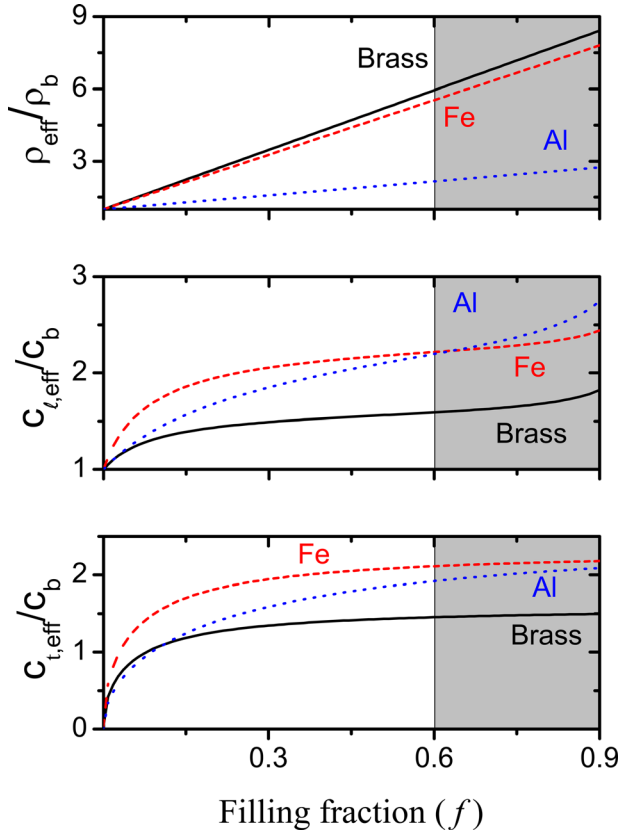
FIG. 3. (Color online) Effective parameters, as in Fig. 2, with olive oil as a background. The effective parameters are normalized to the properties of the fluid background.
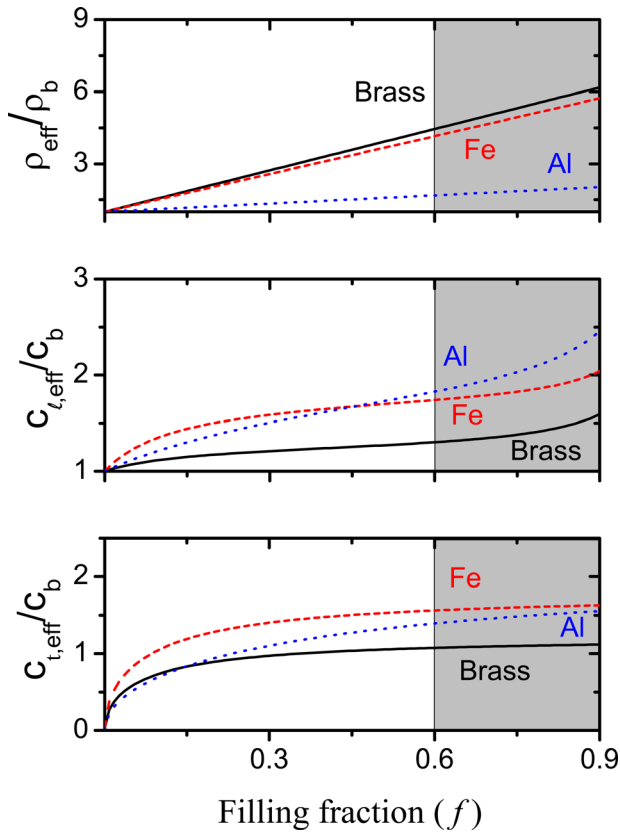

FIG. 4. (Color online) Effective parameters, as in Fig. 2, with glycerin as a fluid background. The effective parameters are normalized to the properties of the fluid background.

TABLE I. Parameters of the fluids used in the calculations. They are taken from Ref. 46.

	Water	Olive oil	Glycerine
ρ_b (Kg/m^3)	998	920	1259
c_b (m/s)	1486	1430	1909
η (Pa · s)	0.001	0.084	0.95

Poisson's ratio is $\sigma = 1 - 2(c_t/c_\ell)^2$ for 2D systems and that values σ larger than 0.5 corresponds to a modulus of rigidity that is small compared with the compression modulus. Values to the right of the arrows correspond to $f \geq 0.6$, where Eq. (36) is not reliable. The velocities of the material cylinders are represented by symbols. Note that, despite of the dilute medium approach, the effective velocities shown in Fig. 5 tend to that of their material constituents as $f \rightarrow 0.9$, the close packing condition of the hexagonal lattice. Note that effective elastic media with ratios c_ℓ/c_t not found in ordinary solids is direct a consequence of the background viscosity here considered.

Although effective parameters in Eq. (35) do not show any explicit dependence on viscosity η, the next section will show that viscosity produces observable effects in the resulting effective medium.

IV. VISCOSITY EFFECTS: RESULTS AND DISCUSSION

Here, we study two selected structures: a single elastic cylinder with circular cross-section and a cluster made of circular elastic cylinders having an external circular shape. Both structures are considered to be immersed in a viscous fluid. First, in Sec. IV A, we analyze the angular distribution of the scattered pressure at the far field for the case in which the viscous fluid is glycerin. Afterwards, in Sec. IV B, we analyze the relative difference of the forward fields by the effective medium and the circular cluster, respectively, in order to establish the homogenization limit. We conclude that viscosity produces observable effects at the far field as well as in the frequency cutoff determining the homogenization limit.

A. Viscosity effects at the far field

The scattered field by a cluster of cylinders is

$$P^{\text{scatt}}(r, \theta) = P_0 \sum_{\alpha=1}^{N} \sum_{q=-\infty}^{\infty} (B_\alpha)_q^\ell H_q(k_\ell r_\alpha) e^{iq\theta_\alpha}. \quad (38)$$

TABLE II. Material properties of the elastic cylinders used in the numerical examples. The elastic parameters are normalized to the corresponding fluid background properties.

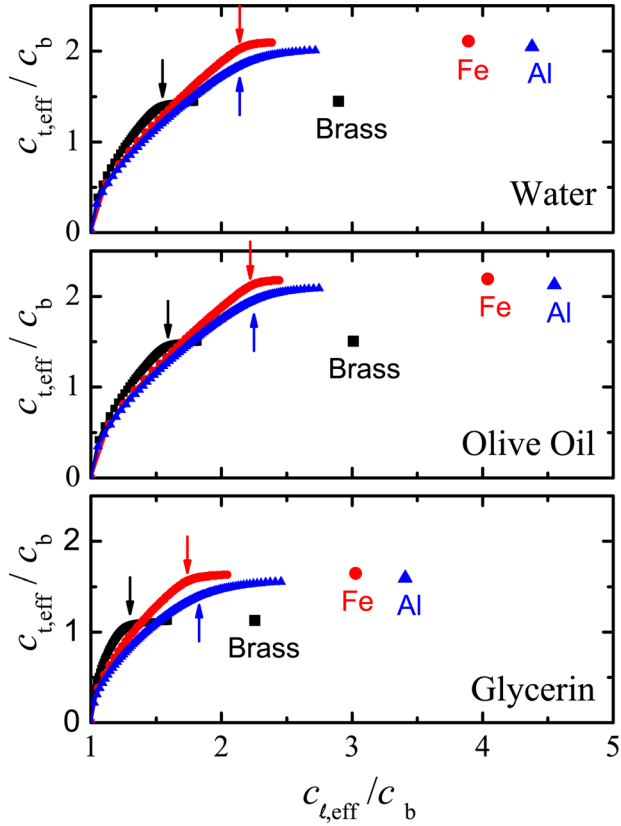|	Water			Olive oil			Glycerine		
	Brass	Fe	Al	Brass	Fe	Al	Brass	Fe	Al
$\bar{\rho}_a$	8.52	7.89	2.70	9.24	8.55	2.93	6.75	6.25	2.14
$\bar{c}_\ell$	2.90	3.89	4.38	2.25	4.04	4.55	2.26	3.03	3.41
$\bar{c}_t$	1.45	2.11	2.05	1.51	2.19	2.13	1.13	1.64	1.59

FIG. 5. (Color online) Phase diagram of the effective phase velocities. The velocities are calculated using expressions obtained for the case of diluted structures (low filling fractions). Values to the right of the downward arrows correspond to filling fractions higher that 0.6, where the calculated values are not reliable. The symbols represent the values of the materials employed in the different structures.
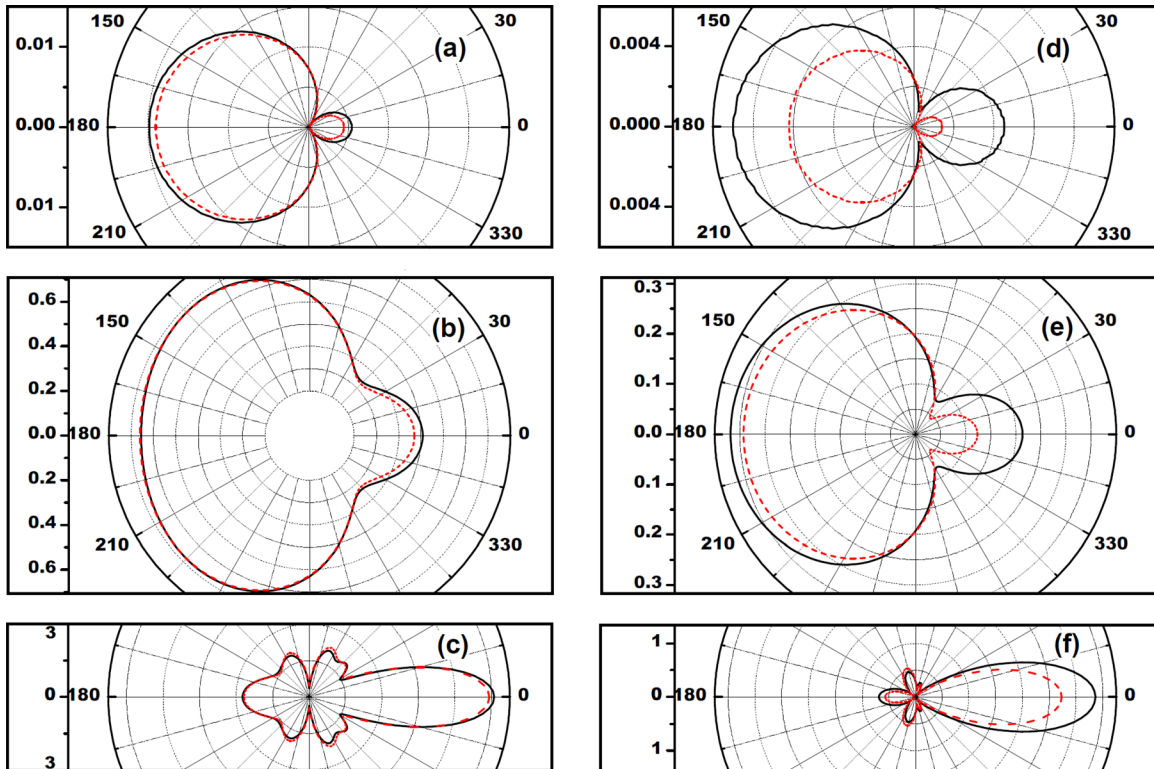
By using the asymptotic form of the Hankel functions for large arguments,[39] the acoustic pressure at the far field is

$$\sigma(k, \theta) \equiv \lim_{r \to \infty} |\sqrt{r} P^{\text{scatt}}(r, \theta)|$$

$$= P_0 \left| \sum_{\alpha=1}^{N} \sum_{q=-\infty}^{\infty} (-i)^q (B_\alpha)_q^\ell e^{-ik_\ell R_\alpha \cos(\theta - \theta_\alpha)} e^{iq\theta} \right|. \tag{39}$$

For the case of a single cylinder this expression is simplified to[36]

$$\sigma(k, \theta) = \left| \sum_{q=-\infty}^{\infty} (-i)^q B_q^\ell e^{iq\theta} \right|. \tag{40}$$

Numerical simulations are performed by considering the case of (i) a brass cylinder with circular cross section and radius $R_a = 794\,\mu\text{m}$ immersed in glycerin and (ii) a circular cluster of 151 brass cylinders distributed in a hexagonal lattice with parameter $a = 794\,\mu\text{m}$ and with radii $R_a = 0.3a$ The cluster radius is $R_{\text{cls}} = 6.452a$, which is obtained by using Eq. (37).

Figure 6 represents the pressure at the far field of both cases for several frequencies. For the single cylinder case it is observed that viscosity only modifies the forward and backward pressure patterns of the pressure when the frequency of the incident wave is increased. A similar result was previously reported by Lin and Raptis.[36] However, note that our result at frequency $kR_a = 5$ slightly differs from that

FIG. 6. (Color online) The scattered far field for a brass cylinder immerse in a glycerin background for different frequencies: (a) $kR_a = 0.1$, (b) $kR_a = 1$, and (c) $kR_a = 5$, and the scattered far field for a cluster of 151 cylinders of brass in glycerin (d) $kR_{\text{cls}} = 0.1$, (e) $kR_{\text{cls}} = 1$, and (f) $kR_{\text{cls}} = 5$; red line (viscous result) and black line (inviscid result).

Reyes-Ayona *et al.*: Homogenization of rods in a viscous fluid   2903

in Fig. 2(c) of Ref. 36. We attribute this difference to better convergence of data obtained here. In our calculations, we have determined that convergence is achieved by including angular momenta up to a certain $q_{\max}$, which is obtained from the following relationship:

$$q_{\max} = q_0 + \frac{k}{N} \sum_{i=1}^{N} R_i, \qquad (41)$$

with N and R_i being the number of cylinders and their radii, respectively. For the frequencies employed in this study it has been found that $q_0 = 3$ ensures good convergence. Then, for the case of a single cylinder $N = 1$ and $kR_a = 5$ the resulting $q_{\max} = 9$.

Regarding the pressure behavior at the far field for the cluster [see Figs. 6(d)–6(f)], the strongest effect of the viscosity is due to additive contributions of losses produced at the surfaces of cylinders.[49] For the frequencies used in the calculation we get a significant viscous penetration depth δ. We can conclude that viscosity plays non-negligible role in the modification of the pressure at the far field, especially along the backward and forward directions. This result is expected since the main amount of energy is essentially concentrated in both directions and, therefore, they are more sensitive to quantify the losses due to viscosity. We have employed this result to consider the forward direction as a reference in order to establish the condition determining the long wavelength limit (homogenization limit) of a circular cluster of elastic cylinders.

B. Homogenization limit for a cluster of elastic cylinders in viscous medium

A wavelength of around four times the lattice parameter has been found as a minimum wavelength in order to reach the homogenization of a cluster of rigid cylinders in an inviscid background.[25,26] However, due to the presence of viscosity in the background as well as the elastic properties of the
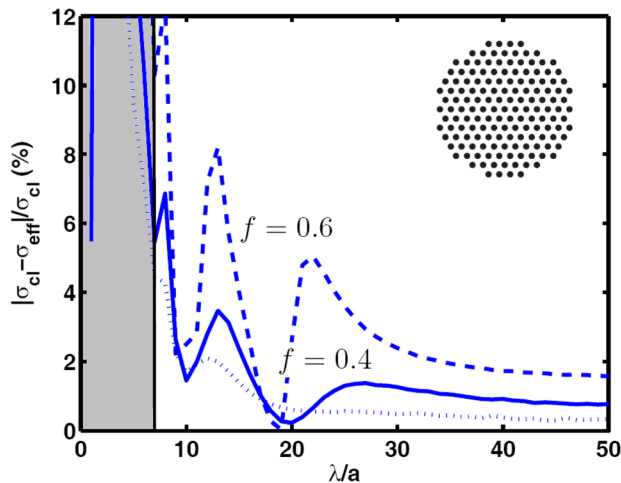

FIG. 7. (Color online) The relative difference between the forward scattering cross section calculated for a cluster of 151 brass cylinders $\bar{\sigma}_{\text{cls}}$ and its corresponding homogenized cylinder σ_{eff} for three filling fraction: $f = 0.2$ (dotted line), $f = 0.4$ (continuous line), and $f = 0.6$ (dashed line).

TABLE III. Effective parameters of hexagonal distributions of brass cylinders embedded in glycerin for several values of filling fraction. They are normalized to the corresponding values of glycerin (see also Fig. 4).

f	$\bar{\rho}_{\text{eff}}$	$\bar{c}_{\ell,\text{eff}}$	$\bar{c}_{t,\text{eff}}$
0.2	2.15	1.172	0.8934
0.4	3.30	1.239	1.0198
0.6	4.45	1.301	1.0755

cylinders it is expected that this cutoff could be slightly different. In fact, it has been shown above how the background viscosity modifies the pressure at the far field at different frequencies.

In order to establish the new limit of homogenization for the viscous-elastic structures under study here we analyze the pressure field distributions produced by a cluster of brass cylinders and its corresponding homogenized cylinder. Particularly, we calculate the forward scattering cross sections as a function of the frequency by using the expressions in Eqs. (39) and (40). Figure 7 reports the relative difference between the forward scattering cross section calculated for the cluster and the corresponding homogenized cylinder σ_{eff} for three different filling fractions; $f = 0.2$, 0.4, and 0.6. The
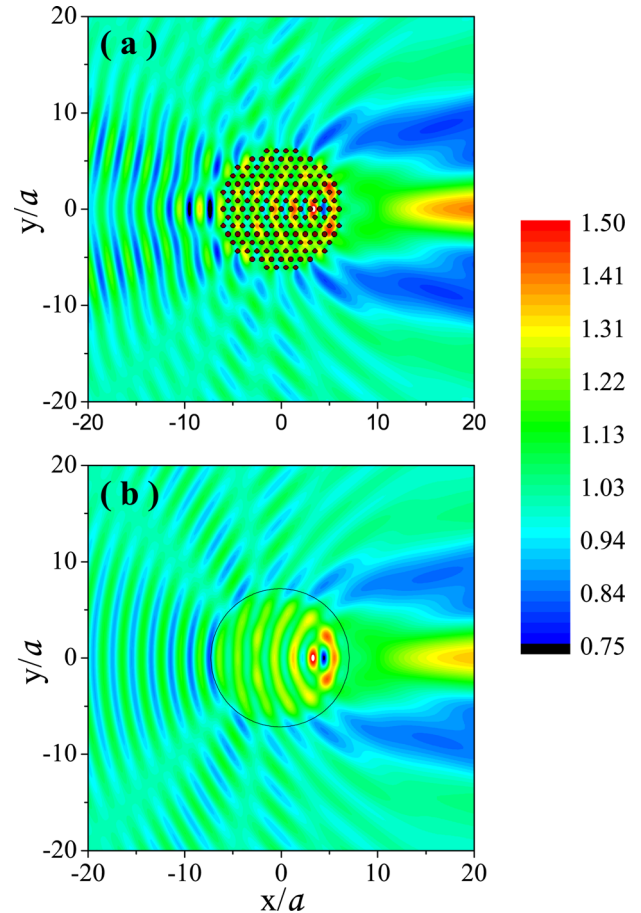

FIG. 8. (Color online) Pressure map (amplitude) representing the scattering of a sound plane wave of wavelength $\lambda = 4a$ interacting with (a) a cluster made of 151 brass cylinders arranged in a hexagonal lattice with filling fraction $f = 0.2$ and embedded in glycerin and (b) the corresponding homogenized cylinder also embedded in glycerin.
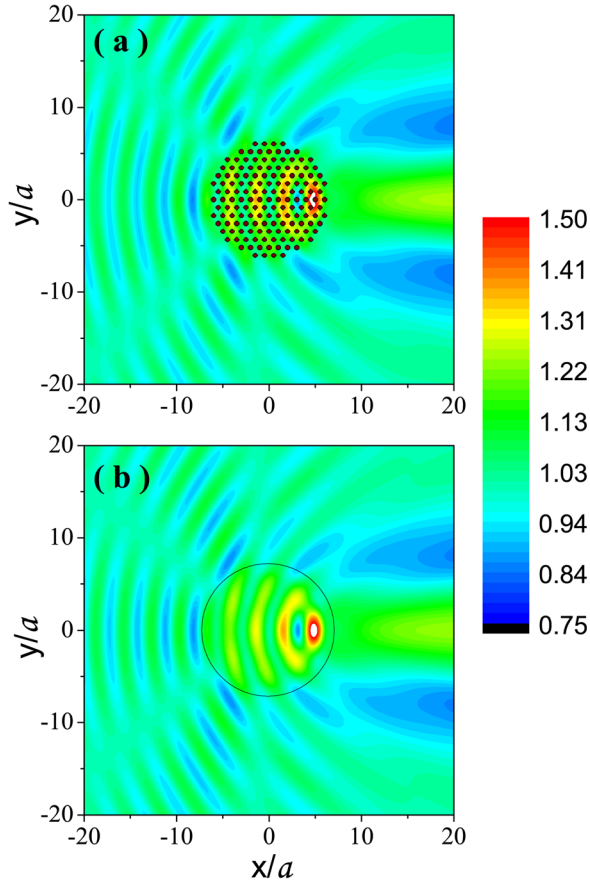
FIG. 9. (Color online) Similar to Fig. 7 but for an impinging wavelength $\lambda = 6a$. Note the good agreement between both pressure maps.

values of effective parameters employed to calculate σ_{eff} are given in Table III. Results in this figure establish that the new homogenization cutoff is around $\lambda = 6a$, where a relative error less than 6% is obtained within the homogenization region for the lower filling fractions.

To support our previous finding, Figs. 8 and 9 depict pressure maps of the scattering of a plane sound wave by a circular cluster of brass cylinders distributed in a hexagonal lattice with $f_{\text{hex}} = 0.2$ and the corresponding homogenized cylinder for $\lambda = 4a$ and $\lambda = 6a$, respectively. From Fig. 7 it is observed that the wavelength $\lambda = 4a$ (the homogenization limit in an inviscid background) is not enough to get a good agreement between both pressure patterns. Unlike this, maps in Fig. 8, which correspond to $\lambda = 6a$, show a fairly good agreement.

Based on these results we conclude that viscosity increases the wavelength cutoff above which the homogenization is achieved.

V. SUMMARY

We have employed the multiple scattering method to analyze the scattering of acoustic waves by a cluster of elastic inclusions embedded in a viscous fluid host. Particularly, we have obtained asymptotic relations of the corresponding t matrix elements in the long wavelengths limit. They are used to derive analytical formulas for the parameters of the effective homogeneous solid representing the cluster in such

a limit. We demonstrated that the effective mass density as well as the effective longitudinal and transversal sound speed depend on the structural distribution of the cylinders, their physical parameters, and the embedded medium. The resulting effective homogenized solid is a kind of elastic metamaterial whose elastic properties can be tailored by changing the cylinders' filling fraction in the cluster. We reported numerical simulations for several elastic-viscous fluid composites that support the validity of the formulas obtained for the effective parameters. It is also found that viscosity produces an increase of minimum wavelength for which the homogenization is achieved in comparison with the case of an inviscid host. We concluded that artificial elastic materials with parameters not found in nature can be obtained by homogenization of clusters made of solid cylinders in a viscous host.

APPENDIX A: t-MATRIX

From Eq. (5), the components of the velocity in the viscous fluid can be expresses in terms of their associated potentials as

$$v_r = -\frac{\partial \varphi}{\partial r} + \frac{1}{r}\frac{\partial \psi}{\partial \theta}, \tag{A1a}$$

$$v_\theta = -\frac{1}{r}\frac{\partial \varphi}{\partial \theta} - \frac{\partial \psi}{\partial r}, \tag{A1b}$$

and those corresponding to the elastic scatterers are

$$v_r = -i\omega\left(-\frac{\partial \phi}{\partial r} + \frac{1}{r}\frac{\partial \zeta}{\partial \theta}\right),$$

$$v_\theta = i\omega\left(\frac{1}{r}\frac{\partial \phi}{\partial \theta} + \frac{\partial \zeta}{\partial r}\right). \tag{A2}$$

These components satisfy the following boundary conditions:

$$v_r^+(R_a) = v_r^-(R_a),$$

$$v_\theta^+(R_a) = v_\theta^-(R_a),$$

$$\sigma_{rr}^+(R_a) = \sigma_{rr}^-(R_a),$$

$$\sigma_{r\theta}^+(R_a) = \sigma_{r\theta}^-(R_a), \tag{A3}$$

where R_a is the radius of the elastic cylinder.

By introducing the expansions of φ_{ext}, φ_{scatt}, ψ_{scatt}, ϕ_{int}, and ζ_{int} in the velocity and after applying the boundary conditions to the resulting expressions, we obtain from the first two conditions in Eq. (A3) that

$$- k_\ell\Big(A_q^\ell J_q'(k_\ell R_a) + B_q^\ell H_q'(k_\ell R_a)\Big) + \frac{iq}{R_a}\Big(B_q^t H_q(k_t R_a)\Big)$$

$$= -i\omega\Big(-k_\ell^a C_q^\ell J_q'(k_\ell^a R_a) + \frac{iq}{R_a}C_q^t J_q(k_t^a R_a)\Big),$$

$$-\frac{iq}{R_a}\Big(A_q^\ell J_q(k_\ell R_a) + B_q^\ell H_q(k_\ell R_a)\Big) - k_t\Big(B_q^t H_q'(k_t R_a)\Big)$$

$$= -i\omega\Big(-\frac{iq}{R_a}C_q^\ell J_q(k_\ell^a R_a) - k_t^a C_{q'}^t J_q'(k_t^a R_a)\Big), \tag{A4}$$

which can be cast in matrix form as

$$\mathbf{M}_q \mathbf{a}_q + \mathbf{N}_q \mathbf{b}_q = \mathbf{O}_q \mathbf{c}_q, \tag{A5}$$

where

$$\mathbf{M}_q = \frac{1}{R_a}\begin{pmatrix} (k_\ell R_a)J_q'(k_\ell R_a) & 0 \\ iqJ_q(k_\ell R_a) & 0 \end{pmatrix}, \tag{A6}$$

$$\mathbf{N}_q = \frac{1}{R_a}\begin{pmatrix} (k_\ell R_a)H_q'(k_\ell R_a) & -iqH_q(k_t R_a) \\ iqH_q(k_\ell R_a) & (k_t R_a)H_q'(k_t R_a) \end{pmatrix}, \tag{A7}$$

$$\mathbf{O}_q = \frac{-i\omega}{R_a}\begin{pmatrix} (k_\ell^a R_a)J_q'(k_\ell^a R_a) & -iqJ_q(k_t^a R_a) \\ iqJ_q(k_\ell^a R_a) & (k_t^a R_a)J_q'(k_t^a R_a) \end{pmatrix}, \tag{A8}$$

and

$$\mathbf{a}_q = \begin{pmatrix} A_q^\ell \\ 0 \end{pmatrix}, \quad \mathbf{b}_q = \begin{pmatrix} B_q^\ell \\ B_q^t \end{pmatrix}, \quad \mathbf{c}_q = \begin{pmatrix} C_q^\ell \\ C_q^t \end{pmatrix}. \tag{A9}$$

Similarly, from the last two boundary conditions in Eq. (A3) we obtain

$$\Delta\Big\{-k_\ell^2\Big(A_q^\ell J_q''(k_\ell R_a) + B_q^\ell H_q''(k_\ell R_a)\Big) + \frac{iqk_t}{R_a}\Big(B_q^t H_q'(k_t R_a)\Big) - \frac{iq}{R_a^2}\Big(B_q^t H_q(k_t R_a)\Big)\Big\}$$

$$+\frac{\Upsilon}{R_a}\Big\{\frac{q^2}{R_a}\Big(A_q^\ell J_q(k_\ell R_a) + B_q^\ell H_q(k_\ell R_a)\Big) - iqk_t\Big(B_q^t H_q'(k_t R_a)\Big) - k_\ell\Big(A_q^\ell J_q'(k_\ell R_a) + B_q^\ell H_q'(k_\ell R_a)\Big) + \frac{iq}{R_a}\Big(B_q^t H_q(k_t R_a)\Big)\Big\}$$

$$= \Delta_a\Big\{-(k_\ell^a)^2 C_q^\ell J_q''(k_\ell^a R_a) + \Big(\frac{iqk_t^a}{R_a}J_q'(k_t^a R_a) - \frac{iq}{R_a^2}J_q(k_t^a R_a)\Big)C_q^t\Big\}$$

$$+\frac{\lambda_a}{R_a}\Big\{\frac{q^2}{R_a}C_q^\ell J_q(k_\ell^a R_a) - iqk_t^a C_{q'}^t J_q'(k_t^a R_a) - k_\ell^a C_q^\ell J_q'(k_\ell^a R_a) + \frac{iq}{R_a}C_{q'}^t J_q(k_t^a R_a)\Big\} \tag{A10}$$

and

$$\eta\Big\{-k_t^2\Big(B_q^t H_q'(k_t R_a)\Big) - \frac{iqk_\ell}{R_a}\Big(A_q^\ell J_q'(k_\ell R_a) + B_q^\ell H_q'(k_\ell R_a)\Big) + \frac{iq}{R_a^2}\Big(A_q^\ell J_q(k_\ell R_a) + B_q^\ell H_q(k_\ell R_a)\Big)$$

$$-\frac{1}{R_a}\Big\{\frac{q^2}{R_a}\Big(B_q^t H_q(k_t R_a)\Big) + iqk_\ell\Big(A_q^\ell J_q'(k_\ell R_a) + B_q^\ell H_q'(k_\ell R_a)\Big) - k_t\Big(B_q^t H_q'(k_t R_a)\Big) - \frac{iq}{R_a}\Big(A_q^\ell J_q(k_\ell R_a) + B_q^\ell H_q(k_\ell R_a)\Big)\Big\}\Big\}$$

$$= \mu_a\Big\{-(k_t^a)^2 C_q^t J_q''(k_t^a R_a) - \Big(\frac{iqk_\ell^a}{R_a}J_q'(k_\ell^a R_a) - \frac{iq}{R_a^2}J_q(k_\ell^a R_a)\Big)C_q^\ell$$

$$-\frac{1}{R_a}\Big\{\frac{q^2}{R_a}C_q^t J_q(k_t^a r) + iqk_\ell^a C_q^\ell J_q'(k_\ell^a R_a) - k_t^a C_{q'}^t J_q'(k_t^a R_a) - \frac{iq}{R_a}C_q^\ell J_q(k_\ell^a R_a)\Big\}, \tag{A11}$$

where

$$\Delta = \xi + \frac{4}{3}\eta + \frac{iB}{\omega}, \quad \Upsilon = \Delta - 2\eta, \quad \Delta_a = \lambda_a + 2\mu_a, \tag{A12}$$

with η, ξ, λ_a, μ_a, and B, being the viscosity constants, the Lamé's coefficients, and the bulk modulus, respectively.

Equations (A10) and (A11) can also be cast in matrix form as

$$\mathbf{P}_q \mathbf{a}_q + \mathbf{Q}_q \mathbf{b}_q = \mathbf{R}_q \mathbf{c}_q, \tag{A13}$$

where

$$\mathbf{P}_q = \frac{1}{R_a^2}\begin{pmatrix} \Delta(k_\ell R_a)^2 J_q''(k_\ell R_a) + \Upsilon[(k_\ell R_a)J_q'(k_\ell R_a) - q^2 J_q(k_\ell R_a)] & 0 \\ 2i\eta q[(k_\ell R_a)J_q'(k_\ell R_a) - J_q(k_\ell R_a)] & 0 \end{pmatrix}, \tag{A14}$$

Reyes-Ayona *et al.*: Homogenization of rods in a viscous fluid

$$\mathbf{Q}_q = \frac{1}{R_a^2} \begin{pmatrix} \Delta(k_\ell R_a)^2 H_q''(k_\ell R_a) + \Upsilon[(k_\ell R_a)H_q'(k_\ell R_a) - q^2 H_q(k_\ell R_a)] & -2i\eta q[(k_t R_a)H_q'(k_t R_a) - H_q(k_t R_a)] \\ 2i\eta q[(k_\ell R_a)H_q'(k_\ell R_a) - H_q(k_\ell R_a)] & \eta[(k_t R_a)^2 H_q''(k_t R_a) - (k_t R_a)H_q'(k_t R_a) + q^2 H_q(k_t R_a)] \end{pmatrix},$$
(A15)

$$\mathbf{R}_q = \frac{1}{R_a^2} \begin{pmatrix} \Delta_a(k_\ell^a R_a)^2 J_q''(k_\ell^a R_a) + \lambda_a[(k_\ell^a R_a)J_q'(k_\ell^a R_a) - q^2 J_q(k_\ell^a R_a)] & -2i\mu_a q[k_t^a R_a J_q'(k_t^a R_a) - J_q(k_t^a R_a)] \\ 2i\mu_a q[(k_\ell^a R_a)J_q'(k_\ell^a R_a) - J_q(k_\ell^a R_a)] & \mu_a[(k_t^a R_a)^2 J_q''(k_t^a R_a) - (k_t^a R_a)J_q'(k_t^a R_a) + q^2 J_q(k_t^a R_a)] \end{pmatrix}.$$
(A16)

It is straightforward to obtain the t-matrix, which relates the coefficients $\mathbf{b}_q$ to $\mathbf{a}_q$, as

$$\mathbf{t}_q = -[\mathbf{Q_q} - \mathbf{R_q O_q^{-1} N_q}]^{-1}[\mathbf{P_q} - \mathbf{R_q O_q^{-1} M_q}], \qquad \text{(A17)}$$

where $[\cdots]^{-1}$ means matrix inversion. Note that t_q is a 2×2 matrix that has the following form:

$$t_q = \begin{pmatrix} t_q^{\ell\ell} & 0 \\ t_q^{t\ell} & 0 \end{pmatrix}. \qquad \text{(A18)}$$

Let us point out that the inverse matrix $[\cdots]^{-1}$ in Eq. (A17) presents singularities associated to its functional dependence on the Hankel functions, which can take values close to zero for certain parameters and frequency regions, where the t-matrix cannot be obtained.

APPENDIX B: LOWER ORDER ELEMENTS OF THE k-EXPANSION OF THE t-SCATTERING MATRIX

The previous appendix has shown that the elements of the t-matrix can be calculated by using the matrix expression (A17), where $\mathbf{t}_{sq} = \mathbf{t}_{qq}\delta_{sq}$. Now, by using the power series expansions of Hankel and Bessel functions for small arguments, is tedious but straightforward to show that the lower order terms of this matrix are

$$\lim_{k\to 0} t_{00}^{\ell\ell} = \frac{i\pi R_a^2}{4} \frac{B_b - B_a}{B_a} \left[1 + ick \frac{(B_b^2\eta - B_a^2\alpha)}{B_b^2 B_a - B_a^2 B_b} \right] k^2 + \vartheta(k^4), \qquad \text{(B1)}$$

$$\lim_{k\to 0} t_{11}^{\ell\ell} = \frac{i\pi R_a^2}{4} \frac{\rho_b - \rho_a}{\rho_b} [B_b - ick\alpha] k^2 + \vartheta(k^4), \qquad \text{(B2)}$$

$$\lim_{k\to 0} t_{22}^{\ell\ell} = \frac{i\pi R_a^2}{4} \mu_a \left[\frac{B_b + 2ick\alpha}{2B_b^2} \right] k^2 + \vartheta(k^4), \qquad \text{(B3)}$$

where $B_a = \lambda_a + \mu_a$ and $\alpha = \frac{4}{3}\eta + \xi$.

In the expressions above we have only considered the longitudinal projection of the $\mathbf{t}_{sq}$ matrix (i.e., $\hat{\ell} \cdot \mathbf{t}_{sq}$), which will be compared with the effective matrix of a cluster of cylinders.

The k-independent factors of lower terms in the power expansion are defined by

$$\hat{t}_{qq}^{\ell\ell} \equiv \lim_{k\to 0} \frac{t_{qq}^{\ell\ell}}{k^2}, \quad q = 0, 1, 2. \qquad \text{(B4)}$$

If we consider clusters of low filling fractions of the inclusions (i.e., the volume occupied by the cylinders is small) the diagonal terms of the effective t−matrix representing the homogenized cluster accomplish that

$$t_{qq}^{\text{eff}} \approx N\hat{\ell} \cdot \hat{\mathbf{t}}_{qq}, \quad q = 0, 1, 2, \qquad \text{(B5)}$$

where N is the number of cylinder and $\hat{\ell} \cdot \hat{\mathbf{t}}_{qq}$ are the lower terms in the power expansion mentioned above. This result is independent of the external shape of the cluster. It is well known that for a cylinder of arbitrary shape, the isotropic element $\hat{t}_{00}^{\text{cyl}}$ is given by

$$\hat{t}_{00}^{\text{cyl}} = \frac{iA_{\text{cyl}}}{4} \left[\frac{B_b}{B_{\text{cyl}}} - 1 \right]. \qquad \text{(B6)}$$

This expression is employed here to describe the isotropic term of an arbitrarily shaped cylinder representing the homogenized cluster with area A_{eff}, and bulk modulus B_{eff}. In other words, it is possible to write Eq. (B5) as

$$\frac{iA_{\text{eff}}}{4} \left[\frac{B_b}{B_{\text{eff}}} - 1 \right] = N \frac{i\pi R_a^2}{4} \left[\frac{B_b}{B_a} - 1 \right], \qquad \text{(B7)}$$

by introducing the filling fraction f as

$$f \equiv \frac{N(\pi R_a^2)}{A_{\text{eff}}}, \qquad \text{(B8)}$$

and after some simplifications, the effective bulk modulus of the homogenized cluster is finally obtained as

$$\frac{1}{B_{\text{eff}}} = \frac{f}{B_a} + \frac{1-f}{B_b}. \qquad \text{(B9)}$$

In what follows we determine ρ_{eff} by using the next diagonal term in the power expansion, which is easily obtained from Eqs. (34) and (B2):

$$\hat{t}_{11}^{\text{eff}} = \frac{i\pi R_{\text{eff}}^2}{4} \frac{\rho_b - \rho_{\text{eff}}}{\rho_b} \approx N\hat{\ell} \cdot \hat{\mathbf{t}}_{11}. \qquad \text{(B10)}$$

Now, inserting the definition of f [see Eq. (B8)] allows one to merge the last equation in

$$\frac{\rho_b - \rho_{\text{eff}}}{\rho_b} = f\left(\frac{\rho_b - \rho_a}{\rho_b}\right). \tag{B11}$$

Solving for ρ_{eff} we get

$$\rho_{\text{eff}} = f\rho_a + (1-f)\rho_b. \tag{B12}$$

Finally, for the third diagonal term, the low filling fraction limit implies

$$\hat{t}_{22}^{\text{eff}} \approx N\hat{\ell} \cdot \hat{t}_{22}, \tag{B13}$$

and from Eq. (B3) it is clear that

$$\mu_{\text{eff}} = f\mu_a. \tag{B14}$$

[1]M. M. Sigalas and E. N. Economou, "Elastic and acoustic wave band structure," J. Sound Vib. **158**, 377–382 (1992).

[2]M. S. Kushwaha, P. Halevi, L. Dobrzynski, and B. Djafari-Rouhani, "Acoustic band structure of periodic elastic composites," Phys. Rev. Lett. **71**, 2022–2025 (1993).

[3]M. S. Kushwaha, P. Halevi, G. Martínez, L. Dobrzynski, and B. Djafari-Rouhani, "Theory of acoustic band structure of periodic elastic composites," Phys. Rev. B **49**, 2313–2322 (1994).

[4]M. S. Kushwaha, "Stop-bands for periodic metallic rods: Sculptures that can filter the noise," Appl. Phys. Lett. **70**, 3218–3220 (1997).

[5]F. R. Montero de Espinosa, E. Jiménez, and M. Torres, "Ultrasonic band gap in a periodic two-dimensional composite," Phys. Rev. Lett. **80**, 1208–1211 (1998).

[6]J. V. Sánchez-Pérez, D. Caballero, R. Martínez-Sala, C. Rubio, J. Sánchez-Dehesa, F. Meseguer, J. Llinares, and F. Gálvez, "Sound attenuation by a two-dimensional array of rigid cylinders," Phys. Rev. Lett. **80**, 5325–5328 (1998).

[7]C. Rubio, D. Caballero, J. V. Sánchez-Pérez, R. Martínez-Sala, F. Meseguer J. Sánchez-Dehesa, and F. Cervera, "The existence of full gaps and deaf bands in two-dimensional sonic crystals," J. Lightwave Technol. **17**, 2202–2207 (1999).

[8]D. Caballero, J. Sánchez-Dehesa, C. Rubio, R. Mártinez-Sala, J. V. Sánchez-Pérez, F. Meseguer, and J. Llinares, "Large two-dimensional sonic band gaps," Phys. Rev. E **60**, R6316–R6319 (1999).

[9]M. M. Sigalas and N. Economou, "Attenuation of multiple-scattered sound," Europhys. Lett. **36**, 241–246 (1996).

[10]M. M. Sigalas and N. García, "Importance of coupling between longitudinal and transverse components for the creation of acoustic band gaps: The aluminum in mercury case," Appl. Phys. Lett. **76**, 2307–2309 (2000).

[11]J. O. Vasseur, P. A. Deymier, B. Chenni, B. Djafari-Rouhani, L. Dobrzynski, and D. Prevost, "Experimental and theoretical evidence for the existence of absolute acoustic band gaps in two-dimensional solid phononic crystals," Phys. Rev. Lett. **86**, 3012–3015 (2001).

[12]Ph. Lambin, A. Khelif, J. O. Vasseur, L. Dobrzynski, and B. Djafari-Rouhani, "Stopping of acoustic waves by sonic polymer-fluid composites," Phys. Rev. E **63**, 066605 (2001).

[13]Z. Liu, C. T. Chan, P. Sheng, A. L. Goertzen, and J. H. Page, "Elastic wave scattering by periodic structures of spherical objects: Theory and experiment," Phys. Rev. B **62**, 2446–2457 (2000).

[14]Y. Chen and Z. Ye, "Acoustic attenuation by two-dimensional arrays of rigid cylinders," Phys. Rev. Lett. **87**, 184301 (2001).

[15]P. A. Martin, "Multiple scattering by random configurations of circular cylinders: Reflection, transmission and effective interface conditions," J. Acoust. Soc. Am. **129**, 1685–1695 (2011).

[16]F. Cervera, L. Sanchis, J. V. Sánchez-Pérez, R. Martínez-Sala, C. Rubio, F. Meseguer, C. López, D. Caballero, and J. Sánchez-Dehesa, "Refractive acoustic devices for airborne sound," Phys. Rev. Lett. **88**, 023902 (2002).

[17]L. Sanchis, A. Håkasson, F. Cervera, and J. Sánchez-Dehesa, "Acoustic interferometers based on two-dimensional arrays of rigid cylinders in air," Phys. Rev. B **67**, 035422 (2003).

[18]M. Kafesaki, R. S. Penciu, and E. N. Economou, "Air bubbles in water: A strongly multiple scattering medium for acoustic waves," Phys. Rev. Lett. **84**, 6050–6053 (2000).

[19]A. A. Krokhin, J. Arriaga, and L. N. Gumen, "Speed of sound in periodic elastic composites," Phys. Rev. Lett. **91**, 264302 (2003).

[20]Z. Hou, F. Wu, X. Fu, and Y. Liu, "Effective elastic parameters of the two-dimensional phononic crystal," Phys. Rev. E **71**, 037604 (2005).

[21]X. Hu and C. T. Chan, "Refraction of water waves by periodic cylinder arrays," Phys. Rev. Lett. **95**, 154501 (2005).

[22]Q. Ni and J. Cheng, "Anisotropy of effective velocity for elastic wave propagation in two-dimensional phononic crystals at low frequencies," Phys. Rev. B **72**, 014305 (2005).

[23]Q. Ni and J. Cheng, "Long wavelength propagation of elastic waves in three-dimensional periodic solid-solid media," J. Appl. Phys. **101**, 073515 (2007).

[24]J. Mei, Z. Liu, W. Wen, and P. Sheng, "Effective mass density of fluid-solid composites," Phys. Rev. Lett. **96**, 024301 (2006).

[25]D. Torrent, A. Håkasson, F. Cervera, and J. Sánchez-Dehesa, "Homogenization of two-dimensional clusters of rigid rods in air," Phys. Rev. Lett. **96**, 204302 (2006).

[26]D. Torrent and J. Sánchez-Dehesa, "Effective parameters of clusters of cylinders embedded in a nonviscous fluid or gas," Phys. Rev. B **74**, 224305 (2006).

[27]A. A. Kutsenko, A. L. Shuvalov, A. N. Norris, and O. Poncelet, "Effective shear speed in two-dimensional phononic crystals," Phys. Rev. B **84**, 064305 (2011).

[28]Y. Wu, Y. Lai, and Z-Q. Zhang, "Effective medium theory for elastic metamaterials in two dimensions," Phys. Rev. B **76**, 205313 (2007).

[29]A. Einstein, *Investigations on the Theory of the Brownian Movement*, edited by R. Furth (Dover, New York, 1956), pp. 1–139.

[30]G. K. Batchelor and J. T. Green, "The determination of the bulk stress in a suspension of spherical particles to order c^2," J. Fluid Mech. **56**, 401–427 (1972).

[31]Rudolf Sprik and Gerard H. Wegdam, "Acoustic band gaps in composites of solids and viscous liquids," Solid State Commun. **106**, 77–81 (1998).

[32]I. E. Psarobas, N Stefanou, and A. Modinos, "Scattering of elastic waves by periodic arrays of spherical bodies," Phys. Rev. B. **62**, 278–291 (2000).

[33]I. E. Psarobas, "Viscoelastic response of sonic band-gap materials," Phys. Rev. B. **64**, 012303 (2001).

[34]M. I. Hussein, "Reduced Bloch mode expansion for periodic media band structure calculations," Proc. R. Soc. London, Ser. A. **465**, 2825–2848 (2009).

[35]M. I. Hussein, "Theory of damped Bloch waves in elastic media," Phys. Rev. B **80**, 212301 (2009).

[36]Wen, H. Lin, and A. C. Raptis, "Acoustic scattering by elastic solid cylinders and spheres in viscous fluids," J. Acoust. Soc. Am. **73**, 736–748 (1983).

[37]S. M. Hasheminjad and R. Sanaei, "Ultrasonic scattering by a fluid cylinder of elliptic cross section, including viscous effects," IEEE Trans. Ultrason. Ferroelectr. Freq. Control **55**, 391–404 (2008).

[38]*Acoustic, Electromagnetic and Elastic Wave Scattering: Focus on the t-matrix Approach—International Symposium held at The Ohio State University, Columbus, Ohio, USA, June 25–27, 1979*, edited by V.K. Varadan and V.V. Varadan (Pergamon Press, New York, 1980), p. 363.

[39]*Handbook of Mathematical Functions*, edited by M. Abramowitz and I. Stegun (Dover, New York, 1972), p. 363.

[40]D. Torrent and J. Sánchez-Dehesa, "Acoustic metamaterials for new two-dimensional sonic devices," New J. Phys. **9**, 323 (2007).

[41]D. Torrent and J. Sánchez-Dehesa, "Anisotropic mass density by two-dimensional acoustic metamaterials," New J. Phys. **10**, 023004 (2008).

[42]D. Torrent and J. Sánchez-Dehesa, "Acoustic cloaking in two dimensions: A feasible approach," New J. Phys. **10**, 063015 (2008).

[43]J. G. Berryman, "Long-wavelength propagation in composite elastic media I. Spherical inclusions," J. Acoust. Soc. Am. **68**, 1809–1819 (1980).

[44]P. A. Martin, A. Maurel, and W. J. Parnell, "Estimating the dynamic effective mass density of random composites," J. Acoust. Soc. Am. **128**, 571–577 (2010).

[45]L. N. Gumen, J. Arriaga, and A. A. Krokhin, "Metafluids with anisotropic dynamic mass," Fiz. Niz. Temp. **37**, 1221–1224 (2011).

[46]*American Institute for Physics Handbook*, 3rd ed. (MacGraw-Hill, New York, 1972), Chaps. 1–3, pp. 93, 105–115, 131–191.

[47]W. J. Parnell, I. D. Abrahams, and P. R. Brazier-Smith, "Effective properties of a composite half-space: Exploring the relationship between homogenization and multiple-scattering theories," Q. J. Mech. Appl. Math. **63**, 145–175 (2010).

[48]D. Torrent and J. Sánchez-Dehesa, "Evidence of two-dimensional magic clusters in the scattering of sound," Phys. Rev. B **75**, 241404(R) (2007).

[49]L. D. Landau, L.P. Pitaevskii, E. M. Lifshitz, and A.M. Kosevich, *Theory of Elasticity* (Pergamon Press, New York, 1997), pp. 11–14.